Nader Nourdanesh
Navid Farrokhi
Farshid Mosaddeghi

ISSN 1333-1124
eISSN 1849-1391

GEOMETRY OPTIMIZATION OF TWO INFINITE PARALLEL PLATES WITH FREE CONVECTION HEAT TRANSFER

Summary

In this study, geometrical optimization of two infinitive plates for the enhancement of heat transfer between the plates is investigated by considering free convection and thermal radiation as heat transfer mechanisms. It is assumed that heat sources with specified length are placed in a linear array with infinitive length on the lower plate. These heat sources are placed at a specified distance between them. Heat flux of the heat sources and the temperature of the upper cold plate are the given data, and the mean temperature of the heat sources, the temperature difference between the upper cold plate and the mean temperature of the heat sources and the Nusselt number are the major parameters for optimizing the geometry of the plates. First, the problem is solved for two familiar geometries: when there exists an upper plate and when it is omitted. Eventually, a situation in which there are vents in the lower and the upper plate is investigated, and the optimum position of these vents as well as their sizes are obtained. The results show that placing vents on the plates can be very effective for enhancing heat transfer from the heat sources. For a particular array of heat sources and vents on the plates, the Nusselt number has the highest magnitude in comparison with other geometries, and consequently, the maximum heat transfer is available.

Key words: *optimization, heat transfer, free convection, thermal radiation*

1. Introduction

Temperature increase and heat transfer are very important in many industrial applications including miniature electronic equipments, and many studies have considered the phenomenon. These include investigating the unsteady interferences [1] or enhancing heat transfer using oscillating or shaking walls in closed environments [2, 3]. These studies are mainly based on independent models of heat flux on a row of distributed heat sources. Rosentblat et al. [4] investigated the convective heat transfer in horizontal layers of incompressible fluid between two parallel rigid plates which are extended infinitely. They concluded that increasing the amplitude and decreasing the frequency of fluctuations of the lower wall temperature leads to a delay in flow field instability. Mantle et al. [5] studied the effects of temperature changes on free convection water horizontal layers heated from the bottom surface. The experiments were performed by changing the temperature on the lower surface, and it was concluded that when the fluctuation amplitude is rather small, the period has no considerable effect on heat transfer. On the other hand, when the fluctuation amplitude becomes larger the period will have severe effects on the heat transfer rate. Unstable convection in cavities with sinusoidal fluctuations of temperature was numerically studied by Lakhal et al. [6] as well as Soong et al. [7]. Fluctuations with large amplitude and low frequency tend to achieve stable state which is in agreement with the work accomplished by Rosenblat et al. Bae et al. [8] performed a time-dependent two-dimensional numerical investigation in a limited rectangular space with separate heaters on one side of the wall. Three heaters were placed on side walls, and the lower heater was turned on and turned off while the two others were constantly working. According to the studies, the vertical wall that is heated separately enhances the heat transfer coefficient in comparison with the completely heated wall. Keyhani et al. [9] and Shu et al. [10] investigated the free convective heat transfer in a rectangular cavity with fluctuating temperature on one of the walls experimentally and numerically. Bazylack et al. [11] numerically investigated natural convection in an enclosure with distributed heat sources. They reported that heat transfer rates and the onset of thermal instability triggering various regimes are governed by the length and spacing of the sources and the width-to-height aspect ratio of the enclosure. Bazylank et al. [12] assumed two parallel walls to be infinitive to eliminate the wall effects. Also, the heaters on the lower surface were assumed to be an infinite array having sine heat flux. They examined the effects of the existing heat sources phase difference, and concluded that wth increasing the amplitude fluctuations, the temperature difference between the cold upper surface and the mean temperature of the heat sources decreases. Also, setting the phase difference among the existing heat sources on the lower surface diminishes the temperature difference and this is a proof that heat transfer from heat sources is enhanced. Cocco Mariani et al. [13] studied natural convection in an enclosure with partial opening. They investigated the effect of heat source position for a Rayleigh number range of 103 to 106. Bilgen et al. [14–18] numerically investigated natural convection in partially open square enclosures with constant heat flux on the wall. They studied the effect of the opening size, the position of the opening, inclination, number of slots and the Rayleigh number.

Although a few researches have investigated geometry parameters of natural convection heat transfer in *2D* enclosures, to the best of the authors' knowledge, no study has investigated the effect of the position of vents and their area simultaneously in order to find an optimum geometry. This issue is examined in the present investigation. In this study, an optimization for decreasing the difference between the cold surface temperature and the mean temperature of the heat sources is presented by changing the geometric shape of *2D* plates. The two plates are assumed infinitely extended, and heat fluxes caused by the heat sources on the lower surface are set to be constant for each case study. After having found the optimum geometry, effects of that geometry for different heat fluxes of the heat sources are compared in two cases: a case with a simple upper plate and a case with the upper plate omitted. The comparison is also performed by changing the temperature of the upper cold plate.

2. Mathematical model

Fig. 1 shows the geometry and boundary conditions of the model which consists of two parallel plates with two heat sources q'' placed on the lower plate. The periodic boundary conditions show that the plates are extended infinitely. The length of the sources and the distance between them are equal to L. The upper plate has the lower temperature T_C and the boundary condition in the space between the installed heat sources on the lower plate is without heat flux ($q''_S = 0$). Also, the upper and the lower plate are non-slipping.

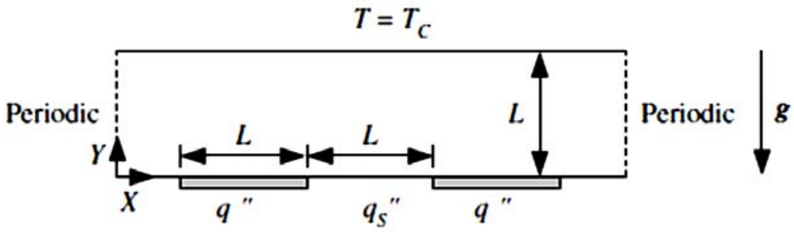

Fig.1 Schematic of 2D geometry and boundary conditions of two parallel plates without vents [11]

In order to optimize the geometry, vents are placed on different locations, and the optimum case would be selected. The case in which the upper plate is eliminated is also investigated for comparison. In this study thermal radiation heat transfer exists as well as convection. It is assumed that the absorption and the scattering coefficients of the air between the two plates are zero. Also, the index of refraction for all wavelengths and for all temperatures is constant and equal to 1. Both plates are opaque and gray-diffuse, with hemispherical emissivity, ε, and absorptivity, α, being the same for both plates. Since after a short period of time, the steady state is reached, the transient terms are omitted in the governing equations. Continuity, momentum and energy equations for this problem are expressed as

$$\nabla \vec{V} = 0 \tag{1}$$

$$\nabla \cdot \left(\vec{V}\vec{V} \right) = -\frac{1}{\rho} \nabla P + \nabla \cdot \left(\nu \nabla \vec{V} \right) + \beta \Delta T \vec{g} \tag{2}$$

$$\rho C_P \left(\vec{V} \cdot \nabla T \right) = k \nabla^2 T \tag{3}$$

where $\vec{V}$, P , ρ , υ, β , g , c_P , k , T are the velocity vector, the static pressure, the density, the kinematic viscosity, the thermal expansion coefficient, the acceleration of gravity, the specific heat, the thermal conductivity and the temperature, respectively. Using the Discrete Ordinates model, the radiative heat transfer equation is solved for temperature, which is the major parameter of the energy equation. The radiation heat transfer equation is expressed as

$$\nabla \cdot \left(I\left(\vec{r}, \vec{s} \right) \vec{s} \right) + \left(\alpha + \sigma_S \right) I\left(\vec{r}, \vec{s} \right) = \alpha n^2 \frac{\sigma T^4}{\pi} + \frac{\sigma_S}{4\pi} \int_0^{4\Pi} I\left(\vec{r}, s \right) \phi\left(\vec{s}, \vec{s}' \right) d\Omega' \tag{4}$$

where I , $\vec{r}$, $\vec{S}$, $\vec{S}'$, α , σ_s , σ, Ω' , Ω are the radiation intensity, the position vector, the direction vector, the scattering direction vector, the absorption coefficient and the scattering coefficient, the Stephan-Boltzmann constant, the phase function and the solid angle, respectively. The internal radiation heat flux from the walls is defined as

$$q''_{in} = \int_{\vec{S}.\vec{n}>0} I_{in} \vec{S} \cdot \vec{n} d\Omega \tag{5}$$

where I_{in} is the intensity of internal radiation, and the net radiative heat flux leaving the wall is expressed as

$$q''_{out} = (1-\varepsilon) q''_{in} + n^2 \varepsilon_w \sigma T_W^4 \tag{6}$$

where ε, T_W are the radiation coefficient of the wall and the wall temperature, respectively. The boundary condition intensity is calculated as follows

$$I_O = \frac{q''_{out}}{\pi} \tag{7}$$

Heat transfer from the heat sources is calculated according to the mean values of the Nusselt numbers on the surface area of the heat sources, and is defined as

$$Nu = \frac{h \cdot L}{k}$$

where L is the characteristic length of the system (as shown in Fig. 1). k is the thermal conductivity, and the heat transfer coefficient h is defined as

$$h(x) = \frac{q''}{T(x) - T_C} \tag{9}$$

The mean Nusselt number is defined as

$$Nu_{av} = \int_0^L Nu(x) dx \tag{10}$$

The Rayleigh number is

$$Ra = \frac{g\beta(T_{\max} - T_C)L^3}{\alpha^* v} \tag{11}$$

where maximum temperature ($T_{\max}$) occurs on the surface of the heat sources, and α^* is the thermal diffusivity of the air.

The convective terms in the transport equations are discretized for solving the equations by using the QUICK scheme. Furthermore, the PRESTO scheme was used to interpolate the pressure values in the steady state solution. A 30×120 uniform quadrilateral mesh which satisfies the grid independency was applied to the computational domain. Further refining the grids did not show considerable effect on the results.

3. Geometry optimization of the two parallel plates

Fig. 2a and Fig. 2b demonstrate the case with the upper plate, and the case when the upper plate is omitted, respectively. $T_{av,s}$ is the mean temperature of the heat sources.

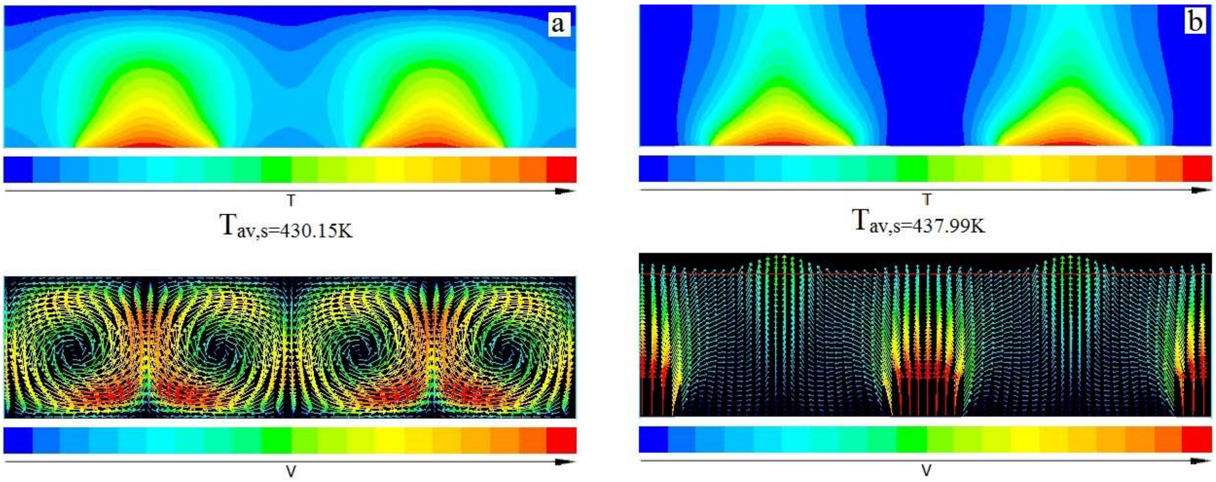

Fig. 2 Contours of temperature and velocity vectors
(a) two parallel plates without vents, **(b)** the upper plates is omitted

As mentioned before, there are few investigations that have studied a similar case study to the one investigated in the current work. Therefore, it is rather hard to find experimental or analytical results to validate the findings of this study. However, the results by Bazylak et al. [12] for the steady state case may be considered to have the similarity in temperature contours.

In order to achieve the optimized geometry of two parallel plates, first vents are created on the lower plate, and then on the upper plate. The best position of the vents in which the maximum temperature ($T_{\max}$) on the heat sources has the minimum value, is concluded. It should be mentioned that in all cases in this section, heat flux of the heat sources is $5000\ \mathrm{W/m^2}$, and the upper plate and the ambient temperature are set to constant values of 273.15K and 300K, respectively. Pressure inlet and pressure outlet are used as boundary conditions at the vents on the lower plate and the upper plate, respectively. The geometry of the optimum array of the vents on the upper plate is shown in Fig. 3.

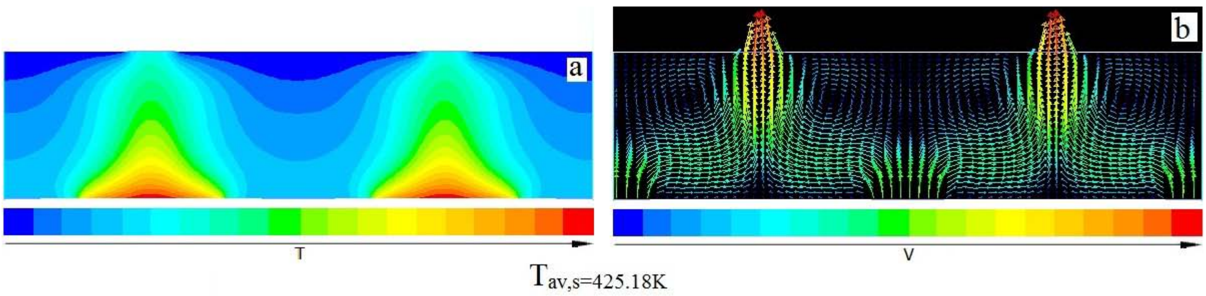

Fig. 3 Obtained case for vents location on the upper plate: a. temperature contour, b. velocity vector.

After the optimized position of the vents on the upper plate is found, this process is repeated for the lower plate to find the optimized condition too. The final optimized geometry is demonstrated in Fig. 4. It is necessary to mention that for the two past processes, the total areas of the vents on the upper and lower plate are set the same in different cases to find the optimum geometry.

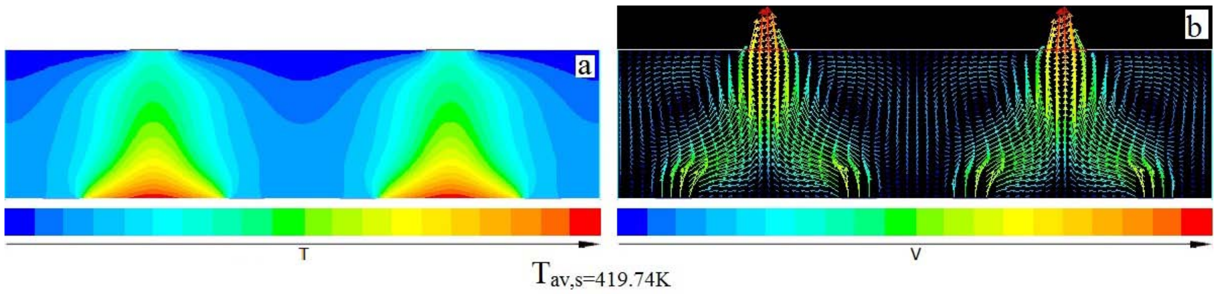

Fig.4 Obtained case for vents location on the lower plate: a. temperature contour, b. velocity vector.

In the next process the area of the vents on the lower and the upper plate is changed in order to find the optimized area of the vents. The optimized geometry obtained in the investigation is shown in Fig. 5.

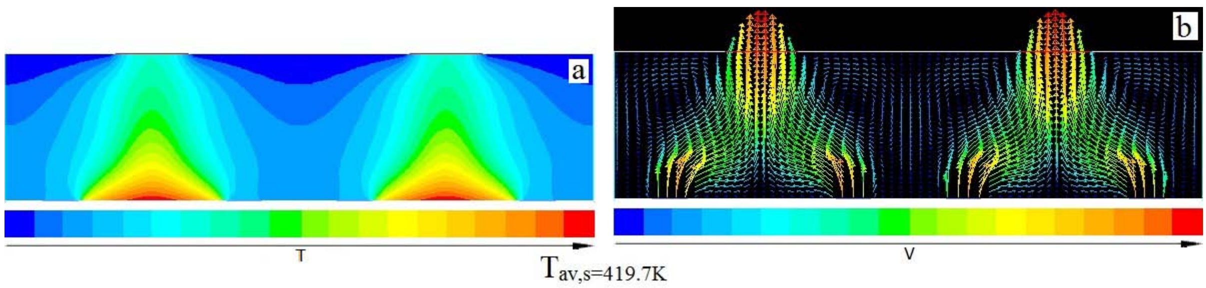

Fig.5 Obtained case for vents area on the upper and lower plates: a. temperature contour, b. velocity vector.

According to the temperature contours and the velocity vectors in Figs. 2-5, it is concluded that decreasing the maximum temperature ($T_{\max}$) by creating and changing the position of the vents causes a change in the velocity vectors between the two plates and the exhaust of the hot air from the vents. In optimized condition, the hot air exits from the upper plate vents, and with creating vortices around the heat sources, the temperature of the air layer on the heat sources decreases leading to the maximum temperature ($T_{\max}$) reduction. Fig. 6 shows the optimum geometry obtained from the mentioned procedures.

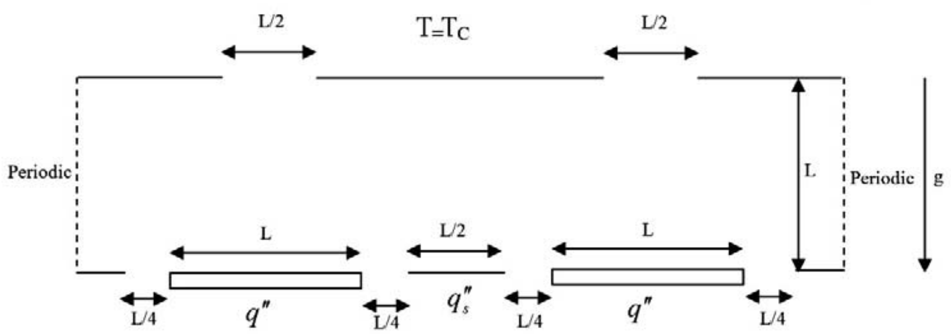

Fig. 6 Schematic of 2D geometry and boundary conditions of two parallel plates for the optimum case

4. Changing the heat flux

In this part of the investigation, the temperature of the cool upper plate is set to be constant (273.15K), and the temperature of the environment is assumed to be 300K. Fig. 7 shows the performance characteristics of the optimized geometry case, the closed case (when the upper plate completely exists) and the open case (when the upper plate is omitted). According to Fig. 7, it can be seen that in the optimized case, $\Delta T_{av,s}$ (the temperature difference between the colder upper plate and the mean temperature on the heat sources) for different heat fluxes is always lower than the corresponding value in the open case. Furthermore, with increasing the heat flux, the temperature difference increases. As shown in Fig. 7a, $\Delta T_{av,s}$ in the optimum case is higher than $\Delta T_{av,s}$ of the closed case. However, with increasing the heat flux, $\Delta T_{av,s}$ related to these two cases converges to a constant value. With further increasing the heat flux (after the convergence point), $\Delta T_{av,s}$ related to the optimum condition becomes lower than the corresponding value in the closed case, and this discrepancy steadily increases. For example, when the heat flux is 5000 W/m^2, $\Delta T_{av,s}$ of the optimum case is 6.9% and 11.1% lower than the value related to the closed and the open case, respectively.

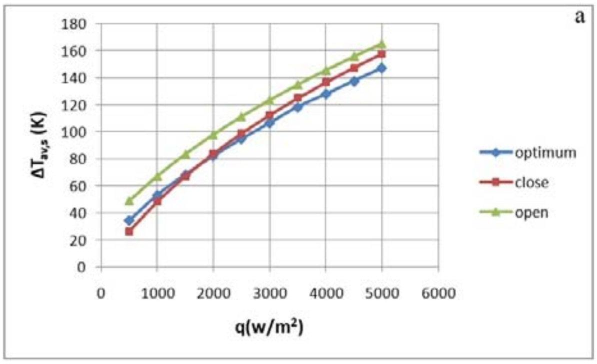

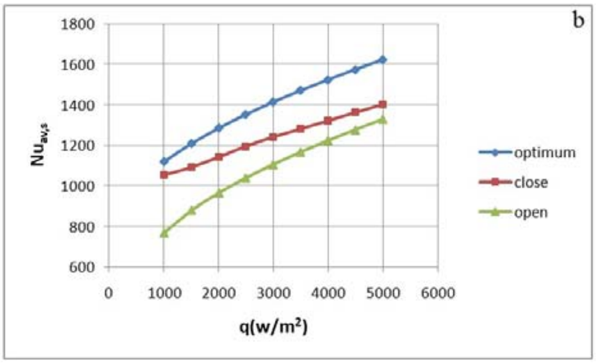

Fig.7 Comparison among close, open and optimum case for different heat fluxes: a. temperature difference between cold plate and heat sources, b. mean Nusselt number at heat sources.

Apparently, enhancement of the heat transfer from the heat sources is shown. From Fig. 7b it is obvious that $Nu_{av,s}$ (the mean Nusselt number at the heat sources) in the optimized case is higher than the two other cases, and with increasing the heat flux in comparison with the open case, this difference is almost constant. However, it increases in comparison with the closed case. As an example, when the heat flux is 5000 W/m^2, in the optimized case $Nu_{av,s}$ increases 15.7% and 22.2% in comparison with the closed and the open case, respectively.

5. Changing temperature of the cold upper plate

In this part, the heat flux of the heat sources is assumed to be constant (2000 W/m^2), and the environment temperature is 300K. Fig. 8 shows the variation of $T_{av,s}$ as a function of temperature changes of the upper plate. According to Fig. 8, it is concluded that for lower temperatures of the colder plate, $T_{av,s}$ (the mean temperature of the heat sources) is higher in the optimum case in comparison with the closed case, but with increasing the wall temperature, this difference decreases, and approaches zero when the temperature of the colder plate is 270K. By further increasing the temperature of the colder plate, this trend continues, and $T_{av,s}$ of the optimum case will be lower than the corresponding value of the closed case. For instance, when the heat flux is 2000 W/m^2 and the temperature of the colder plate is assumed to be equal with the environment temperature (300K), $T_{av,s}$ of the optimum case is significantly (13.3%) lower in comparison with the closed case. Also it decreases 10.6% in comparison with the open case. Fig. 8b demonstrates that for lower temperatures of the colder plate, $Nu_{av,s}$ of the optimum case is lower in comparison with the closed case, but with increasing the temperature of the colder plate this difference is reduced, and eventually it will be higher than the corresponding value of the closed case. For example, when the temperature of the colder plate is equal to the environment temperature (300K), $Nu_{av,s}$ of the optimum case is higher 22% and 17.5% in comparison with the closed and the open case ($Nu_{av,s}$ is 965.2).

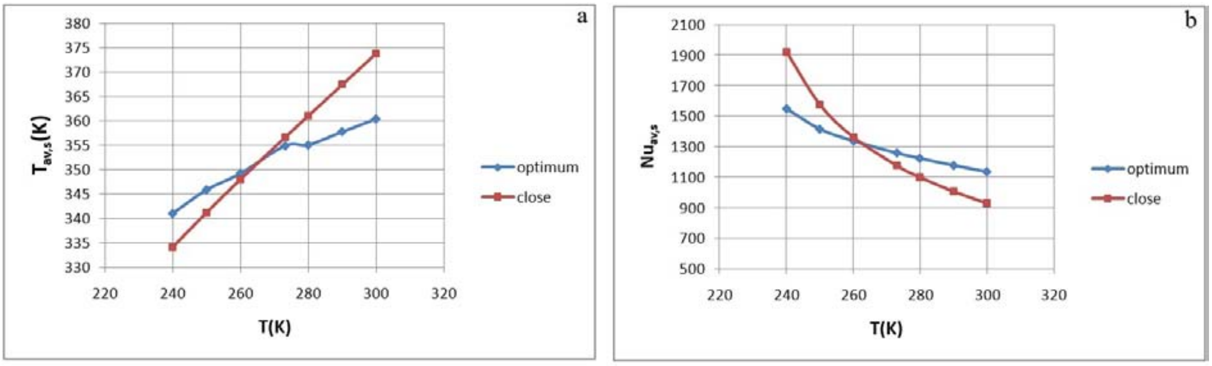

Fig.8 Comparison between close and optimum case for different temperatures of cold plate with heat flux=2000w/m^2: a. mean temperature on heat sources, b. mean Nusselt number on heat sources.

Table 1, demonstrates percentages of the reduction in $\Delta T_{av,s}$ and the increase in $Nu_{av,s}$ for the optimum geometry in comparison with the other geometries. It shows considerable decrease in $\Delta T_{av,s}$ and increase in $Nu_{av,s}$ caused by making appropriate vents on the two plates.

Table 1 Variations of $\Delta T_{av,s}$ and $Nu_{av,s}$ for optimum geometry in comparison with close and open case (Ambient temperature is set to 300K)

Increase in $Nu_{av,s}$ for optimum geometry, %		Decrease in $\Delta T_{av,s}$ for optimum geometry, %		Cold upper plate temperature, K	Heat flux W/m^2
Open	Close	Open	Close		
30.2	7	16.25	2.1	273.15	2000
17.5	22	10.6	13.3	300	2000
22.2	15.7	11.1	6.9	273.15	5000

6. Conclusion

Based on the results of this study, it can be concluded that a special geometrical shape of the bodies (here two infinitive parallel plates) can be very effective for the transfer of heat from heat sources. Therefore, the current investigation presents an optimum geometry. The mean temperature of the heat sources, the difference between the cold plate temperature and the mean temperature of the heat sources and the mean Nusselt number at the heat sources were studied as functions of the heat flux and temperature variations of the cold plate. The results showed that temperature differences between the cold plate and the mean temperature of the heat sources in the optimum case are lower than in other cases for a vast range of operation temperatures. In addition, the mean Nusselt number at the heat sources for optimum case is higher than the other mentioned cases. Reducing the temperature difference between cold plate and mean temperature of the heat sources means that the heat transfer from the heat sources is enhanced which is of great importance for many industrial applications.

REFERENCES

[1] M.J. Vesligaj, C.H. Amon, Transient thermal management of temperature fluctuations during time varying workloads on portable electronics, IEEE Trans. Comp. Pack. Technol. 22 (4) (1999) 541–550.

[2] L.A. Florio, A. Harnoy, Feasibility study of unconventional cooling of electronic components by vibrating plates at close proximity, Numer. Heat Transfer, Part A: Appl. 47 (2005) 997–1024.

[3] C. H. Cheng, K. S. Hung, Numerical prediction of thermal convection in a rectangular enclosure with oscillating wall, Numer. Heat Transfer, Part A: Appl. 48 (2005) 791–809.

[4] S. Rosentblat, G.A. Tanaka, Modulation of thermal convection instability, Phys. Fluids 14 (7) (1971) 1319–1322.

[5] J. Mantle, M. Kazmierczak, B. Hiawy, The effect of temperature modulation on natural convection in a horizontal layer heated from below: high-Rayleigh-number experiments, J. Heat Transfer 116 (1994) 614–620.

[6] E.K. Lakhal, M. Hasnaoui, P. Vasseur, E. Bilgen, Natural convection in a square enclosure heated periodically form part of the bottom wall, Numer. Heat Transfer, Part A: Appl. 27 (1995) 319–333.

[7] C.Y. Soong, P.Y. Tzeng, C.D. Hsieh, Numerical study of bottomwall temperature modulation effects on thermal instability and oscillatory cellular convection in a rectangular enclosure, Int. J. Heat Mass Transfer 44 (2001) 3855–3868.

[8] J.H. Bae, J.M. Hyun, Time dependent buoyant convection in an enclosure with discrete heat sources, Int. J. Therm. Sci. 43 (2004) 3–11.

[9] M. Keyhani, V. Prasad, R. Cox, An experimental study of natural convection in a vertical cavity with discrete heat sources, J. Heat Transfer 100 (1988) 616–624.

[10] Y. Shu, B.Q. Li, B.R. Ramaprian, Convection in modulated thermal gradients and gravity: experimental measurements and numerical simulations, Int. J. Heat Mass Transfer 48 (2005) 145–160.

[11] A. Bazylak, N. Djilali, D. Sinton, Natural convection in an enclosure with distributed heat source, Numer. Heat Transfer, Part A 49 (2006) 655–667.

[12] A. Bazylak, N. Djilali, D. Sinton, Natural convection with distributed heat source modulation, Int. J. Heat Mass Transfer 50 (2007) 1649–1655.

[13] V. C. Mariani, A. Silva, Natural convection: analysis of partially open enclosures with an internal heated source, Numer. Heat Transfer, Part A 52 (2007) 595–619.

[14] E. Bilgen, H. Oztop, Natural convection heat transfer in partially open inclined square cavities, Int. J. Heat Mass Transfer 48 (2005) 1470–1479.

[15] E. Bilgen, A. Balkaya, Natural convection on discrete heaters in a square enclosure with ventilation ports, Int. J. Heat Fluid Flow 29 (2008) 1182–1189.

[16] E. Bilgen, A. Muftuoglu, Cooling strategy by mixed convection of a discrete heater at its optimum position in a square cavity with ventilation ports, Int. Commun. Heat Mass Transfer 35 (2008) 545–550.

[17] E. Bilgen, A. Muftuoglu, Natural convection in an open square cavity with slots, Int. Commun. Heat Mass Transfer 35 (2008) 896–900.

[18] A. Muftuoglu, E. Bilgen, Natural convection in an open square cavity with discrete heaters at their optimized positions, Int. J. Therm. Sci. 47 (2008) 369–377.

Submitted: 14.7.2014

Accepted: 10.6.2015

Nader Nourdanesh
nader.nourdanesh88@ tabrizu.ac.ir
Young Researchers and Elite Club, Ilkhchi Branch, Islamic Azad University, Ilkhchi, Iran

Navid Farrokhi
n.farrokhi@tabrizu.ac.ir
Young Researchers and Elite Club, Ilkhchi Branch, Islamic Azad University, Ilkhchi, Iran

Farshid Mosaddeghi
Department of Mechanical Engineering, Faculty of Mechanical Engineering, University of Tabriz, Tabriz, Iran